HOKKAIDO UNIVERSITY

Title	Self-assembled formation of uniform InP nanopore arrays by electrochemical anodization in HCl based electrolyte
Author(s)	Sato, Taketomo; Fujino, Toshiyuki; Hasegawa, Hideki
Citation	Applied Surface Science, 252(15), 5457-5461 https://doi.org/10.1016/j.apsusc.2005.12.085
Issue Date	2006-05-30
Doc URL	https://hdl.handle.net/2115/14591
Type	journal article
File Information	ASS.pdf

Self-Assembled Formation of Uniform InP Nanopore Arrays by Eelectrochemical Anodization in HCl based Electrolyte

Taketomo Sato, Toshiyuki Fujino and Hideki Hasegawa

Research Center for Integrated Quantum Electronics (RCIQE) and Graduate School of Information Science and Technology,
Hokkaido University, North-13, West-8, Kita-ku, Sapporo, 060-8628, Japan
Fax: +81-11-716-6004, E-mail: taketomo@rciqe.hokudai.ac.jp

Abstract
Attempts were made to optimize the electrochemical anodization process for formation of high-density, regular and straight nanopore arrays on InP. The structure, shape and size of the pores were very sensitive to substrate orientations, electrolyte concentrations and anodization voltages. Among (111)A, (111)B and (001) substrate orientations, the most uniform and most straight nanopore arrays were obtained on (001) substrates at anodization voltages of 5-7 V by using 1.0 - 1.5 M HCl electrolyte containing HNO_3 .The pore depth could be controlled up to 80 μm by the anodization time.

1. Introduction

Recently, various methods for self-assembled formation of nanostructure arrays have been intensively studied in view of applications to electronic devices, photonic devices, photonic crystals[1], chemical and biochemical sensors [2] etc. In III-V semiconductors, traditional approaches for forming nanostructures have been to utilize expensive molecular beam epitaxy (MBE) or metal-organic vapor phase epitaxy (MOVPE) equipments. A possible alternative approach is to apply electrochemical processes directly to semiconductors, similarly to porous Si structures[3]. The features of the electrochemical process are low temperature process, low process damage, and process simplicity and low cost. They can also realize the unique structures such as high density nanopores having high aspect ratio, that are not obtainable by other methods. Several groups have reported on porous structures made of III-V semiconductor materials [4-6]. Recently, we have also succeeded in anodic formation of arrays of straight nanopores on n-InP substrates, using HCl based electrolytes [7-9].

Based on this, the purpose of this paper is further to optimize the anodization process by investigating the detailed dependence of the nanopore structure, density, lateral uniformity and vertical straightness on the substrate orientations, electrolyte concentrations and anodization voltages.

2. Experimental

A simple three-electrode cell was used [7]. It had an n-type InP electrode, a Pt counter electrode and a reference saturated calomel electrode (SCE) and was controlled by a potentiostat. As the InP electrode, n-type substrates with (111)A, (111)B and (001) orientations were prepared in order to investigate the orientation dependence. The doping density was kept the same for all the substrates, being 1×10^{18} cm^{-3}. A GeAu/Ni ohmic contact was made on the backside of the InP substrate by using the conventional metal evaporation and annealing process. In all the experiments, the overpotential was supplied in d.c. mode in the dark.

Based on our previous work [9], a mixture of HCl and HNO_3 was chosen as the electrolyte. To investigate the effect of electrolyte concentration, the following four kinds of

electrolyte, A-D, with different HCl concentrations were prepared, keeping the same proportion of HCl:HNO$_3$.

A: 1.5 M HCl 200ml + HNO$_3$ 4.5ml
B: 1.0 M HCl 200ml + HNO$_3$ 3ml
C: 0.5 M HCl 200ml + HNO$_3$ 1.5ml
D: 0.25M HCl 200ml + HNO$_3$ 0.75ml

3. Results and Discussion

3.1 Basic cyclic voltammetry study

Basic anodic reactions on the n-InP electrode were first investigated by cyclic voltammetry. Examples of measured typical cyclic voltamographs obtained for n-InP (001) electrodes are shown in **Fig. 1**. They showed typical behavior of the active-passive transition Namely, below a certain critical overpotential, uniform anodic dissolution took place. However, above this critical value, active-passive transition took place, and formation of oxides and nanopore arrays started. As seen in **Fig. 1**, the magnitude of anodic currents changed with the electrolytes. However, the critical overpotential remained constant. The magnitude of anodic current density, J, was also strongly dependent on the crystal orientations. In the present experiments, the relation of $J_{111B} > J_{111A} > J_{001}$ was always observed for the same electrolyte.

3.2 Dependence of pore morphology on anodization conditions

Surprisingly wide varieties of surface and cross-sectional structures were obtained by changing the conditions, as shown below. This is remarkable if one thinks of the fact that the most basic electrochemical reaction is the same. Main observations are listed below.
(1) There is a minimum electrolyte concentration for formation of pore structures. When the electrolyte was too dilute, only continuous and rather nonuniform anodic oxide without pores was formed as shown in **Fig. 2(a)** for the electrolyte D. It suggests that pore formation is initiated by the attack on the oxide by Cl$^-$ and/or NO$_3^-$ ions in the electrolyte.
(2) When pores were formed, the structure generally consisted of the top irregular region including the surface oxide layer and the pore region underneath, as schematically shown in **Fig. 2(b)**. The thickness of the top irregular region was typically 500 nm to 1 μm, whereas the thickness of the underlying pore region depended on the anodization conditions and could become longer than 80 μm.
(3) Pore shapes seen on the plan views of the surface depended strongly on the substrate orientation. For example, the arrays of pores having a triangular shape were formed both on (111)A and (111)B substrates as shown in **Fig. 3(a)** and **(b)**. The triangles were aligned in the same direction with three sides being parallel to three equivalent <-110>-orientations. On the other hand, square shape pores defined by {100} planes were formed on the (001) substrate, as shown in **Fig. 3(c)**. Under certain conditions, interesting self-organized regular patterns appeared on the (001) surface as shown in **Fig. 3(d)**. All these features indicate that initial attack on the oxide is sensitive to chemical nature of the surface.
(4) Cross-sectional structures of the pore region depended strongly on the substrate orientations, electrolyte concentrations and anodization voltages. Main structures included chaotic pore patterns shown in **Fig. 4(a)**, tree-like pore structures, zig-zag pores shown in **Fig. 4(b)**, vertical winding pores and vertical straight pores shown in **Fig. 4(c)** and **(d)**.

General features can be roughly explained in terms of two different competing tendencies. One is to form pores in the preferential directions of weak bonds that are easily attacked by the electrolyte. This tendency is enhanced in more concentrated electrolytes. The other is the tendency of forming straight pores along the direction of electric field which is producing holes required for reaction by impact ionization. This tendency is enhanced at larger anodization voltages.
(5) The lateral structures of the pore region are generally different from the plan view pore

structures shown in **Fig. 3(a)-(d)**. An example is shown in **Fig. 5(a)** for a (001) case where the irregular top layer of the sample shown in **Fig.3(c)** was peeled off. It is seen that a quasi-periodic array of square pores with an average size of 110 nm are formed. In this case, the size and period of pores did not change with time, but could be controlled by the applied anodization bias. Another example is shown in **Fig. 5(b)** where (111)B- oriented pore walls are missing due to over-etching in a concentrated electrolyte of 1.5 M. Thus, the irregular top layer is the transition layer in which the lateral structure of the pore region is determined by increase of pore diameter caused by supply of holes and chemical dissolution. The former is eventually self-limited by depletion of holes in the pore wall.

(6) Among three substrate directions, the (001) direction was found to be most suitable for forming uniform and straight nanopore arrays such as shown in **Fig. 4(c)** and **(d)**. This in very different from the case of Si, GaAs and other reports on InP [3-6]. Suitable electrolyte concentrations are 1.0 M to 1.5 M and suitable anodization voltages are 5-7 V.

3.3 Pore depth control

For applications, the pore depth and its controllability are very important. The measured pore depth is plotted vs. electrolyte concentration in **Fig. 6(a)**. For all the substrate orientations, the pore depth increased with increase of HCl concentration and saturated around 1.0 M. This result suggests that the vertical reaction velocity becomes rate-limited at some concentration by supply of holes in the InP electrode rather than the transport of reaction by-products in the electrolyte.

The observed anodization time dependence is shown in **Fig. 6 (b)**. The solid curve with a right axis indicates the current density measured during the anodization. Initially, the pore depth increased rapidly, and then, increased linearly with time. This result is consistent with the behavior of the anodic current. From these results, the pore depth can be controlled by the anodization time.

4. Conclusion

In the anodic formation of nanopores in InP, the pore structure, shape and size are surprisingly sensitive to substrate orientations, electrolyte concentrations and anodization voltages. Among (111)A, (111)B and (001) substrate orientations, the most uniform and most straight nanopore arrays were obtained on (001) substrates at anodization voltages of 5-7 V by using 1.0 - 1.5 M HCl electrolytes containing HNO_3. The pore depth could be controlled up to 80 μm by the anodization time.

References
[1] C. Jamois, R. B. Wehrspohn, L. C. Andreani, C. Hermann, O. Hess and U. Gösele: Photonics and Nanostructures-Fundamentals and Applications, **1** (2003) 1.
[2] Y. Wand, Z. Tang and N. A. Kotov: Materials Today, **8** (2005) 20.
[3] R. L. Smith, S.-F. Chuang and S. D. Collins: J. Electron. Mater., **17** (1988) 533.
[4] T. Takizawa, S. Arai, M. Nakahara, Jpn. J. Appl. Phys., **33** (1994) L643.
[5] M. Hao, H. Uchida, C. Shao, T. Soga, T. Jimbo and M. Ueno: J. Cryst. Growth, **179** (1997) 661.
[6] S. Langa, I. M. Tiginyanu, J. Carstensen, M. Christophersen and H. Föll: Appl. Phys. Lett., **82** (2003) 278.
[7] A. Hamamatsu, C. Kaneshiro, H. Fujikura and H. Hasegawa: J. Electroanal. Chem., **473** (1999) 223.
[8] H. Fujikura, A. Liu, A. Hamamatsu, T. Sato and H. Hasegawa: Jpn. J. Appl. Phys., **39** (2000) 4606.
[9] H. Hasegawa and T.Sato: Electrochimica Acta **50** (2005) 3015.

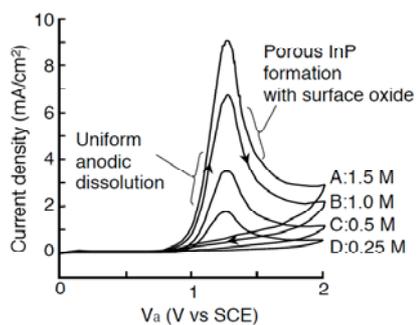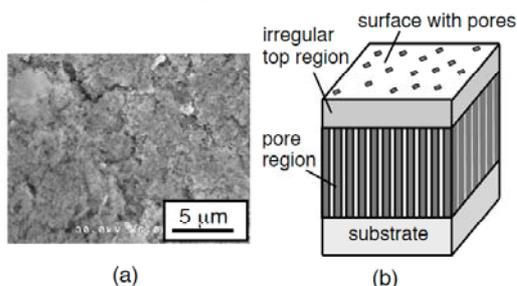Fig.1 Cyclic voltamograms on (001) InP surface.

(a)   (b)

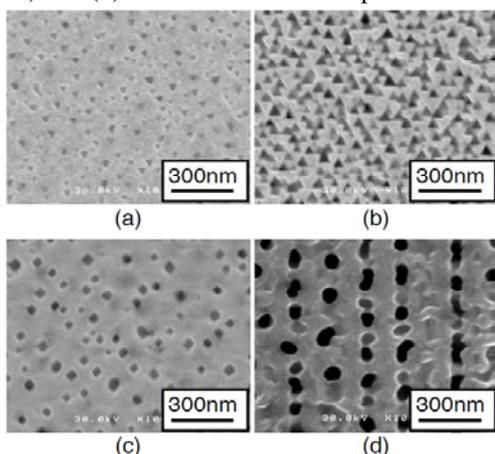Fig.2 (a) Plan view of InP surface without pores (001, D, 5V) and (b) structure of anodized pores.

(a)   (b)

(c)   (d)

Fig.3 Plan view of surfaces. (a)(111)A , A , 3 V, (b) (111)B, A , 1V, (c) (001), B , 5V and (d) (001), C, 5V.
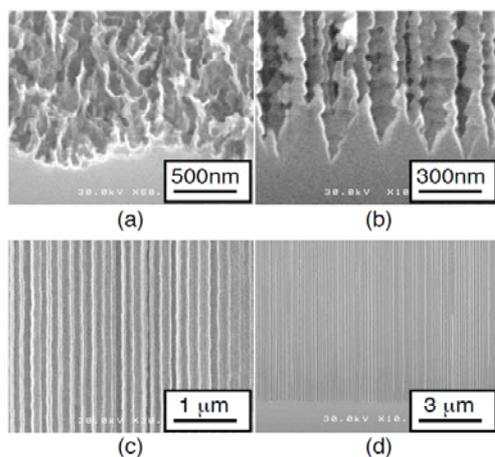

(a)   (b)

(c)   (d)

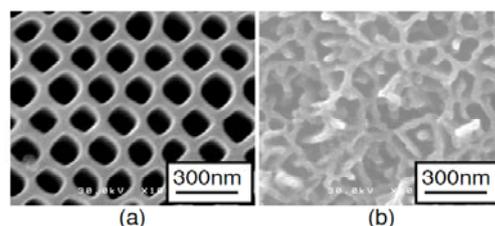Fig.4 Cross-sectional structure of pore region. (a) (111)A, B, 3V,(b) (111)B, B, 1V (c) and (d) (001), B, 5V.

(a)   (b)

Fig.5 Plan view of pore region (a)(001), B , 5V and (b) (111)B, A , 5V.
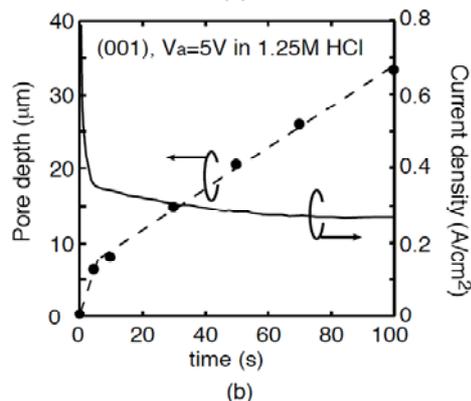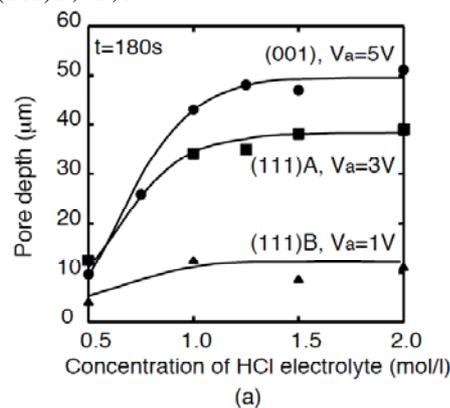

(a)

(b)

Fig.6 (a) Measured pore depth as a function of the HCl concentration. (b) Pore depth and the anodization current vs. time.